

OBSERVATION AND ANALYSIS OF MICROTREMORS UNDERGROUND

by

Teiji TANAKA^I and Kaio OSADA^{II}

ABSTRACT

Underground observation of microtremors in the frequency range of 1 to 10 c/s was made in a bore-hole, 42 m deep, to study the characteristics of short-period microtremors with special emphasis on the identification of their waves-types. Change in amplitude and phase with depth was examined from simultaneous records both at ground surface and underground by means of the power- and cross-spectra. Through the comparison between the observed and theoretical results, the horizontal component of microtremors is shown to consist mainly of S waves, the fundamental mode Rayleigh waves and /or the first higher mode Love waves. It is also shown that the microtremors can be treated as the multiple reflection phenomena of S waves in the subsoil layers, for the convenience of engineering applications.

INTRODUCTION

Microtremors have been widely recognized as a useful and convenient tool for obtaining information on the transfer characteristics of subsoil layers to seismic waves. However, for reasonable prediction of the spectral feature of earthquake ground motions from microtremor data, it is necessary to know the types of waves of which the microtremors are composed. Although, much research along this line has been carried out, so far, it has not yet become clear mainly because of the complexity of their mechanism of generation.

One of the approaches to this problem is the detailed examination of the amplitude distribution of microtremors underground. The repeated observation of microtremors at successively increased depths was carried out in a bore-hole, 42 m in depth, at the site of the Earthquake Research Institute, where P- and S-wave velocity data are available. Using the records at 17 different depths, change in amplitude and phase of microtremors with depth was obtained by means of the power- and cross-spectra. The observed amplitude distribution in the subsoils was interpreted through the comparison with those expected theoretically for S(multiple reflections)-, Love- and Rayleigh waves to identify the wave-types of the microtremors. The main objective of this study is to ascertain the result of our previous studies [1] that the principal part of microtremors can be treated as a multiple reflection phenomenon of S-waves in the surface layers, for the sake of convenience of practical application to engineering purposes.

SOIL CONDITIONS AND METHOD OF OBSERVATION

The subsoil profile and standard penetration resistance values (N-value) observed in the hole are shown in Fig. 1. Velocity distribution of

I Lecturer, II Research associate, Earthquake Research Institute, University of Tokyo.

P- and S-waves obtained by velocity logging at a distance of a few meters [2] is also shown in Fig. 1.

The observation system used to record microtremors is composed of bore-hole seismometers, amplifiers with an integrating circuit and an FM magnetic data recorder. The seismometer is a TUSS type bore-hole seismometer (two horizontal components, $T_0 = 0.3$ sec) with a shunt condenser so as to extend apparently the natural period of pendulum. The overall frequency characteristics of the system are almost flat for ground displacement in the range from 1 to 10 c/s. The sensitivity and frequency characteristics of the two seismometers were calibrated relatively by simultaneous recording at the ground surface.

The observation points were arranged at intervals of 1 m to 5 m so that the distance increases with depth as illustrated by a black circle in Fig. 1. In the observation, two horizontal components of microtremors were recorded simultaneously at the surface and at the bottom of a hole. As the hole was dug deeper and deeper, the observation was completed by repeating this process 16 times from a depth of 1 m to 42 m. Errors in direction of the seismometer setting between the surface and hole were estimated to be less than 5 degrees. Observation was made carefully in the daytime and a record was taken at each depth for 15 minutes.

RESULTS OF OBSERVATION

Some of the examples of microtremor records are shown in Fig. 2. The amplitude level of microtremors during the observation was about 0.5 microns at the surface. In Fig. 2, the close similarity of the records from two seismometers at the surface (0 m) and a rapid decrease of high-frequency components of the waves with depth are clearly seen. The root-mean-square (r.m.s.) amplitudes were computed from the 60 sec samples at each depth and the ratio of the hole to surface is shown in Fig. 3. The r.m.s. amplitudes for two horizontal directions are almost the same. A remarkable feature found in the figure is that the amplitude decreases very rapidly down to about 10 m and becomes nearly constant at greater depths. To witness the phase difference between the records at the surface and hole, the cross-correlations were computed. The results are shown in Fig. 4. All the correlograms have the highest value at a lag equal to zero and this indicates that the microtremors, as a whole, are an almost completely random phenomenon, at least in this case.

In the computation of the power- and cross-spectra, the sample length and the maximum lag in the correlation function were chosen to be 60 sec and 5 sec, respectively, to obtain meaningful spectra. Fig. 5 illustrates the power spectra obtained from the records at the surface and at different depths. Fig. 6 shows the amplitude ratio (square root of the power ratio) of the hole spectrum to surface spectrum for NS component. It is noted again that the amplitude ratios between the two spectra at the surface are almost unity over the frequency range under consideration. The lowest value of the amplitude ratio occurs at a frequency of around 5 c/s for depths deeper than 7.6 m. The upper part of Fig. 7 shows the average amplitude spectra computed from 17 records at the surface obtained by repetition of the observation. The lower part of Fig. 7 shows the average spectrum for all 34 component records together with a range of $\pm 1\sigma$. In the figure,

significant peaks are seen at frequencies of 1.8, 3.3 and 5.3 c/s.

Fig. 8 shows the normalized amplitude distribution under the ground for the above three predominant frequencies. The solid line in the figure represents the mean amplitude distribution of the two components, NS and EW. As will be shown later, since the observed phase difference has a value between 0 and $\pm\pi$ radians, the amplitudes are plotted in an absolute value. The pattern of decreasing in wave amplitude with depth is strongly dependent on the frequency as expected from the wavelength of each component waves. The amplitude of waves of 5 c/s frequency decreases very rapidly from the surface down to about 10 m. This indicates that the 5 c/s waves are closely related with the soil layers of loam and clay whose S-wave velocities are relatively low.

In an attempt to interpret the above amplitude distribution in more detail, the cross-correlations were computed from the records at depths of 0 m and 13 m, and 0 m and 27.4 m after digital band-pass filtering. Fig. 9 shows the cross-correlograms for the pass-band of 1.5 to 2.5 c/s and 4.5 to 5.5 c/s. The correlograms indicate that the waves of 2 c/s frequency at a depth of 27.4 m are almost in-phase with those at the surface, while for the waves of 5 c/s the phase are nearly opposite to the surface. The phase difference for waves of different frequencies was obtained from the co- and quad-spectrum of which the cross-spectrum is formed. Fig. 10 shows the result for NS component. The phase difference at the surface (0 m) represents a good agreement of the phase characteristics between the two seismometers. The general feature seen in Fig. 10 is that lower the frequency of the waves, the deeper the depth becomes to turn the phase to opposite. The gradual change in the phase from 0 to $-\pi$ represents the viscoelastic properties of the soil layers.

COMPARISON BETWEEN THE OBSERVED AND THEORETICAL RESULTS

In order to identify the type of waves present in the microtremors, the transfer characteristics of the subsoil layers to each of the S-, Love- and Rayleigh waves were calculated using the wave velocity data shown in Fig. 1. Fig. 11 shows the observed amplitude ratios between the spectra at depths of 0 m and 12.95 m, and the theoretical amplitude ratios for the multiple reflections of S waves at vertical incidence. The observed amplitude ratios have their maximum at a frequency of around 5.3 c/s, while peaks in the theoretical curves appear at significantly lower frequencies than the observed one. The broken line shown in Fig. 10 represents the theoretical phase differences obtained for the multiple reflections of S waves, assuming the Q value of 20 for all the soil layers. In the figure, the theoretical curves are also shift systematically to the low frequency side. This discrepancy may be due to the unsuitable velocity structure model used in the calculations.

Since waves of about 5 c/s frequency which predominate at the surface are of particular interest, only the theoretical amplitude distribution for this frequency is shown in Fig. 12. In Fig. 13, the theoretical and observed results are compared in an absolute value. So far as the amplitude distribution near the surface is concerned, all the theoretical results are explainable of the observed ones in a general sense. However, as seen in Fig. 10, for the waves of about 5 c/s frequency, the phase angle at the sur-

face becomes almost opposite to that at a depth of 27 m. This fact strongly suggests the possibility that the significant part of microtremors at this site were composed mainly of S waves, the fundamental mode of Rayleigh waves and /or the first higher mode of Love waves.

Fig. 14 shows the directional distribution of the power spectral densities ($f = 5.2$ c/s) at the surface estimated from the power- and cross-spectral density functions for the two horizontal components of microtremors at five different days. The patterns of spectral density distribution in the figure are difficult to explain by only one type of waves coming from one directions.

As additional data, results of comparison of the spectra between the microtremors (velocity) and earthquake ground motions (acceleration) observed at the site of E. R. I. are illustrated in Fig. 15. The spectra of microtremors are the results obtained at two places at a distance of 90 m, and that of earthquake motion is the average of 12 accelerograms observed at one of the places. Apart from a slight shift of the microtremor spectra to higher frequency range, both spectra are in good agreement.

CONCLUDING REMARKS

Through the dense underground observation of microtremors, some of the waves present in the microtremors have been identified. The results indicate that the horizontal component of microtremors in the frequency range of 1 to 10 c/s mainly consist of S waves, the fundamental mode Rayleigh waves and /or the first higher mode Love waves. Probably, they consist of a mixture of these types of waves. Although the waves most attributable to the short-period microtremors could not be distinguished, it was ascertained more that the observed results could be interpreted in general even if we assume that they depend only on the multiple reflection phenomena of S waves in the subsoil layers.

In conclusion, the authors wish to thank Dr. K. Kudo for his valuable suggestions and permission in making the computer programs of the surface waves available.

REFERENCES

1. Kanai, K., T. Tanaka and S. Yoshizawa, 1965, On Microtremors. IX. (Multiple Reflection Problem), Bull. Earthq. Res. Inst., 43, 577-588.
2. Kudo, K. and E. Shima, 1970, Attenuation of Shear Waves in Soil, Bull. Earthq. Res. Inst., 48, 145-158.

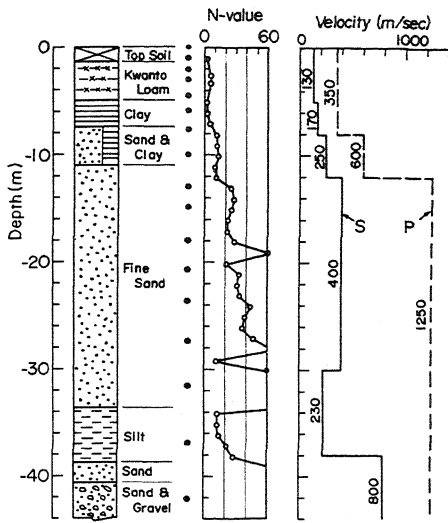


Fig. 1. Subsoil profile and distribution of N-values and wave velocities.

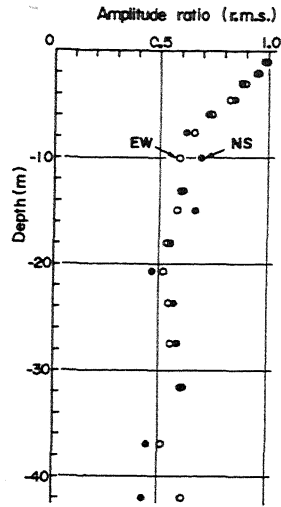


Fig. 3. The root-mean-square amplitude ratios with depth.

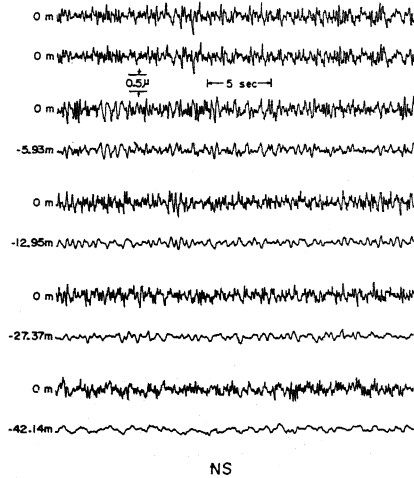


Fig. 2. Examples of microtremors records. NS component.

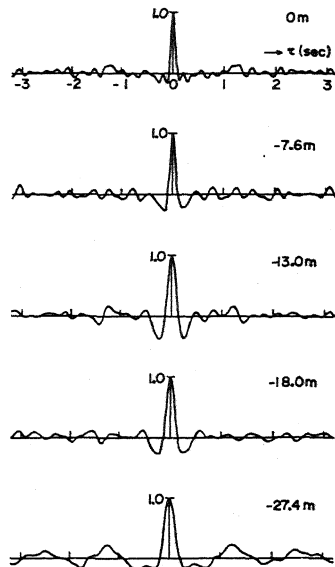


Fig. 4. Cross-correlations between the microtremors at the surface and at different depths.

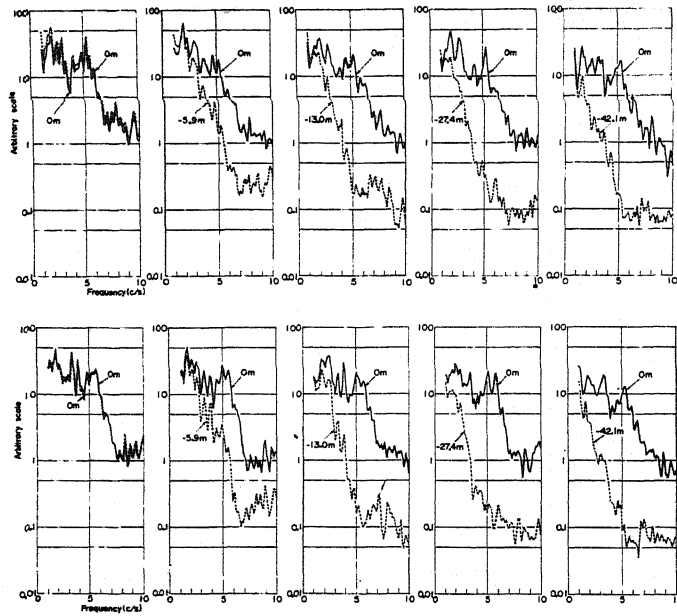


Fig. 5. Power spectra of microtremors at different depths under the ground. Upper; NS component, Lower; EW component.

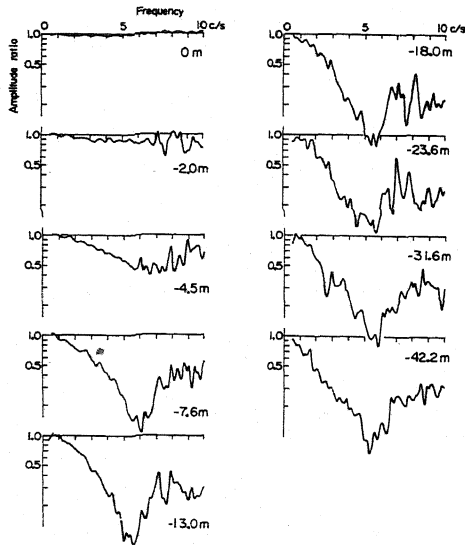


Fig. 6. Amplitude ratios of the underground spectrum to the surface spectrum. NS component.

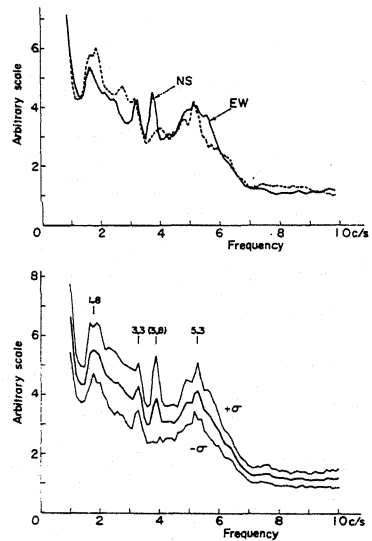


Fig. 7. Average amplitude spectrum (square root of the power spectral density) of microtremors at the surface.

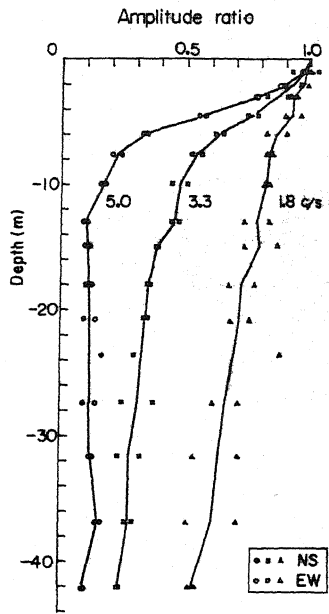


Fig. 8. Spectral amplitude ratios with depth for frequencies of 1.8, 3.3 and 5.0 c/s.

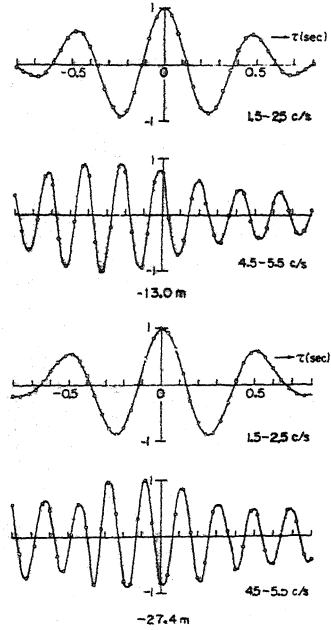


Fig. 9. Cross-correlations between the band-pass filtered microtremors at depths of 0 m and 13 m, and 27.4 m.

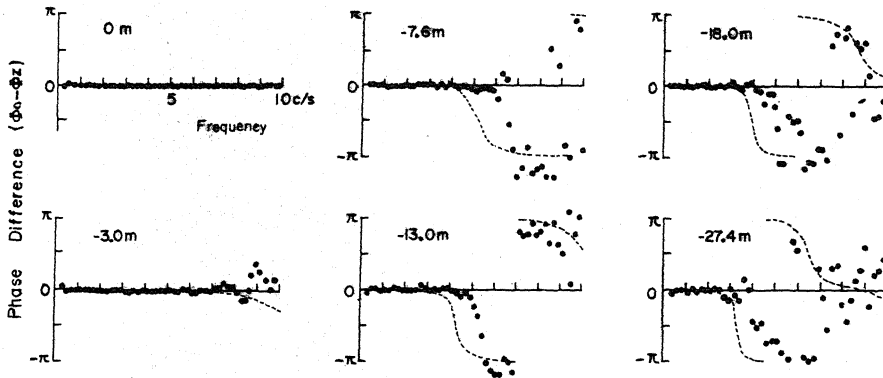


Fig. 10. Phase differences between the microtremors at the surface and underground.

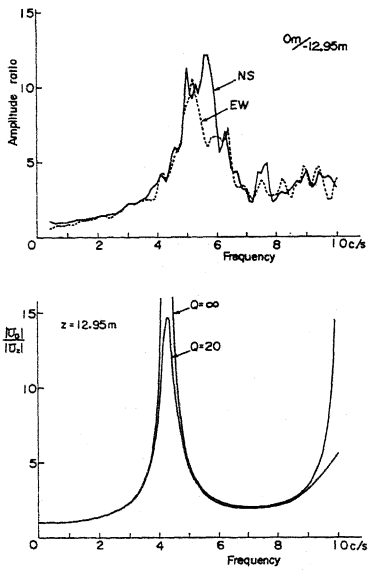


Fig. 11. Observed amplitude ratios of the microtremors at the surface and a depth of 12.95m (uppermost) and the theoretical results for S waves.

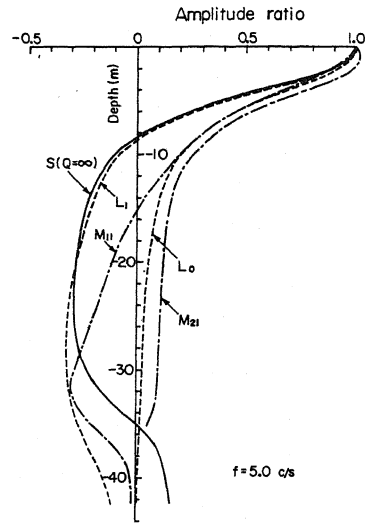


Fig. 12. Theoretical amplitude distribution for SH, Love and Rayleigh waves.

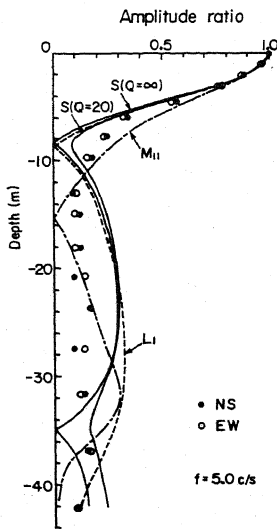


Fig. 13. Comparison of the observed and theoretical amplitude distribution for a frequency of 5.0 c/s.

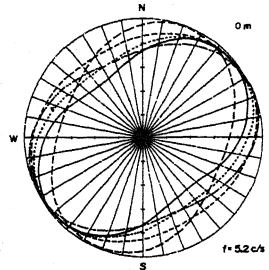


Fig. 14. Directional distribution of the power spectral density of microtremors.

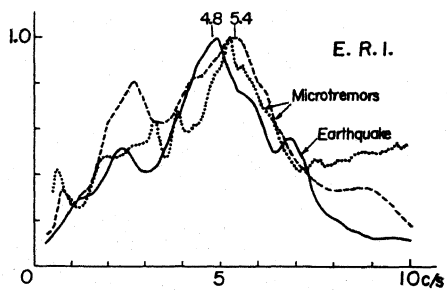


Fig. 15. Comparison of the average amplitude spectra of microtremors (velocity) and earthquake motions (acceleration).